ARTICLE

OBC
www.rsc.org/obc

Multistate properties of 7-(*N*,*N*-diethylamino)-4′-hydroxyflavylium. An example of an unidirectional reaction cycle driven by pH

Margarida C. Moncada,[a,b] Damián Fernández,[a] João C. Lima,[a] A. Jorge Parola,[a] Carlos Lodeiro,[a] Filipe Folgosa,[a] M. João Melo[c] and Fernando Pina*[a]

[a] *REQUIMTE/CQFB, Departamento de Química, Faculdade de Ciências e Tecnologia, Universidade Nova de Lisboa, 2829-516 Monte de Caparica, Portugal. E-mail: fjp@dq.fct.unl.pt*

[b] *Instituto Superior de Ciências da Saúde, Monte de Caparica, Portugal*

[c] *REQUIMTE/CQFB, Departamento de Conservação e Restauro, Faculdade de Ciências e Tecnologia, Universidade Nova de Lisboa, 2829-516 Monte de Caparica, Portugal*

Received 18th June 2004, Accepted 30th July 2004
First published as an Advance Article on the web 13th September 2004

The synthetic flavylium salt 7-(*N*,*N*-diethylamino)-4′-hydroxyflavylium tetrafluoroborate gives rise in aqueous solution to a complex network of chemical reactions driven by pH. The system was studied by ^{1}H NMR, single crystal X-ray diffraction, steady state and transient UV-Vis spectrophotometry as well as stopped flow. The crystal structure shows a high degree of coplanarity between the pyrylium system and the phenyl group in position 2. Thermodynamic and kinetic constants for the pH dependent network of chemical reactions were obtained. The introduction of an amino group in position 7 allows formation of protonated species leading, in particular, to a tautomeric form of the protonated *cis*-chalcone, $\mathbf{CcH}^+$, whose absorption spectra is rather red shifted, in comparison with the correspondent protonated *trans*-chalcone, $\mathbf{CtH}^+$. The $\mathbf{CcH}^+$ species can be rapidly converted into the flavylium cation through a first order process with lifetime of 0.2 s at pH = 2.35. This new reaction channel confers this compound a peculiar behaviour in acidic media, allowing to define an unidirectional pH driven reaction cycle.

Introduction

Generation, detection, transfer and storage of chemical signals (semiochemistry)[1] is a subject of increasing interest. The importance of signal manipulation becomes unquestionable, when biological processes are considered. Communication, and by consequence manipulation of signals, is a vital process in all the complex machinery of the living organisms.

At the molecular-level, multistate chemical systems, in particular those exhibiting photochromic properties, can be the physical support for the manipulation of the chemical signals, and for this reason they have been subjected to a systematic investigation.[2–6] Multistate systems can respond, upon different stimuli, from a pulse of light, or a pH jump to the addition of ions. Such kind of systems have been used, for example, to conceive optical memories, and molecular scale logic gates.[1–3] Taking living systems as an example, the possibility of using protons as stimuli, is something that can stimulate our ingenuity in order to introduce new ideas and concepts. The use of proton stimuli to achieve a chemical response of a multistate system is the main aim of the present work.

Several multistate systems have been reported in literature, namely those based on diarylethenes,[4] fulgides,[5] and spiropyranes.[6] In contrast, the rich and complex network of chemical reactions involving synthetic flavylium salts was object of less interest.[2a]

The network of chemical reactions in which synthetic flavylium salts are involved is now firmly established. Synthetic flavylium salts possess the same basic structure and exhibit identical chemical behaviour of anthocyanins, the ubiquitous colorants of flowers and fruits. Probably due to their similarity with anthocyanins, and because Nature is prodigal in its creativity, the network of chemical reactions involving synthetic flavylium salts shows great versatility depending on the nature and position of substituents. On the basis of our accumulated knowledge on the chemical behaviour of several synthetic flavylium salts,[2,7] a flavylium salt bearing a protonable diethylamino group in position 7 was synthesized, allowing to extend the network of chemical reactions to protonated amino species, Scheme 1. The various species shown, as well as the intricate network of chemical reactions in which they participate, will be characterized throughout this work.

Results and discussion

Synthesis and characterization

The synthesis of 7-(*N*,*N*-diethylamino)-4′-hydroxyflavylium tetrafluoroborate was achieved through the acid catalysed condensation of 4′-hydroxyacetophenone with 4-(diethylamino)-salicylaldehyde, following a method early introduced by Robinson[8] and slightly modified by Katritzky *et al.*[9]

The ^{1}H NMR spectra was carried out in D_2O. When the solution is acidified to pD < 0.6 with DCl, the observed spectrum is compatible with the existence of a single species, where full assignment of the signals was possible (see Experimental part) on the basis of scalar coupling constants and by comparison with published spectra of similar 4′,7-disubstituted flavylium salts.[10,11] Taking into account that the pK_a of $\mathbf{AH}_2^{2+}$ is ~−0.67, (see below) the observed spectrum actually corresponds to a mixture of $\mathbf{AH}_2^{2+}$ and $\mathbf{AH}^+$ in fast proton exchange equilibrium. When the D_2O solution is basified with NaOD to pD = 12.7, the spectrum is again compatible with the existence of a single species. This species corresponds to doubly-ionized *trans*-chalcone, $\mathbf{Ct}^{2-}$, on the basis of the large scalar coupling constant between protons 3 and 4 on the double bond of the chalcone ($^3J_{H3–H4}$ = 15.2 Hz) and taking into account that p$K_a(\mathbf{Ct}^-)$ = 9.2 (see below). Full assignment of this spectrum was again possible (see Experimental part).

Crystal structure

Red–green single crystals of 7-(*N*,*N*-diethylamino)-4′-hydroxyflavylium tetrafluoroborate suitable for X-ray analysis were obtained by slow diffusion of diethyl ether into a solution of the compound in acetonitrile–water (10 ml). The crystal structure of this compound is shown in Fig. 1.

Fig. 1 shows the front (A) and side (B) views of the structure of 7-(*N*,*N*-diethylamino)-4′-hydroxyflavylium tetrafluoroborate.

DOI: 10.1039/b409260k

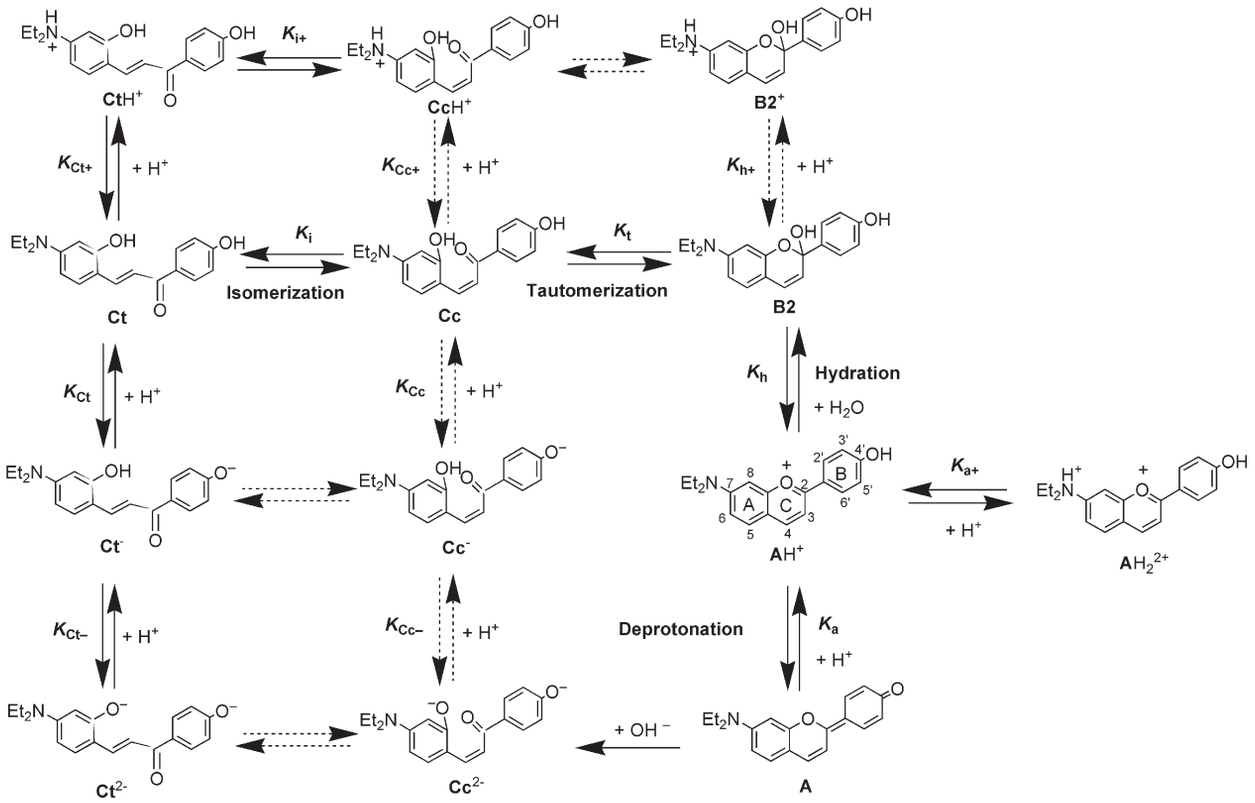

Scheme 1

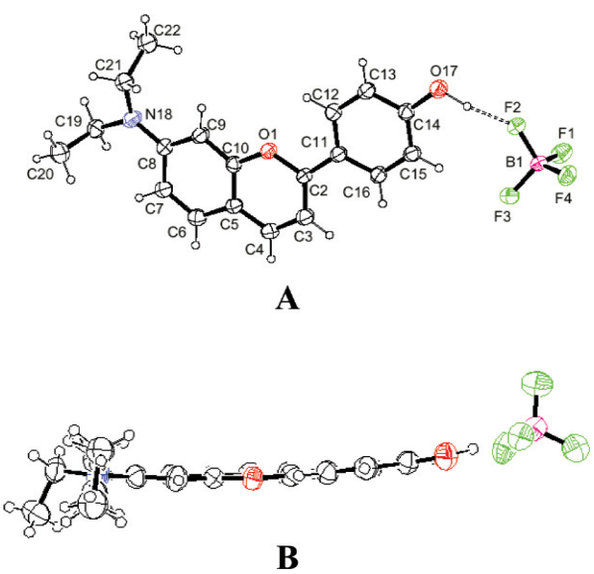

Fig. 1 ORTEP view of the molecular structure of 7-(*N*,*N*-diethylamino)-4′-hydroxyflavylium tetrafluoroborate. Front view with atom label numbers (A) and side view (B). Only the major part of the disorder is shown. Ellipsoids are shown with 50% of probability.

The torsion angle between the benzopyrylium system and the benzene ring is 5.9°, in accordance with the fact that there are no substituents in the position 3 (C3), 2′ (C12) and 6′ (C16), allowing good coplanarity of both aromatic systems in the structure. It is interesting to compare this result with those observed in other flavylium salts. Following the same rule, in the case of 4′-aminoflavylium hexafluorophosphate,[12] a torsion angle of 2.3° was observed, and for 7,8-dihydroxyflavylium chloride[13] and 4′,6,7-trihydroxyflavylium chloride,[14] torsion angles of 0.6° and 5.9°, respectively, were reported. When a methyl group is present in position 4 (C4), the angle increases to 8.1°, as observed in 7,8-dihydroxy-4-methyl flavylium chloride,[13] and when a hydroxyl group or the bulkier methyl group is present in the position 3 (C3), the angle increases, respectively, to 10.1° and 40.4°, as observed in cyanidin bromide (3,5,7,3′,4′-pentahydroxyflavylium bromide)[14] and 3-methylflavylium tetrafluoroborate.[15] This clearly demonstrates the influence of substituents at position 3 (C3) on preventing the coplanarity between the benzopyrylium system and the phenyl at position 2 (C2).

The presence of an amino group at position 7 (C8) allows direct conjugation with the benzopyrylium ring. Since nitrogen is less electronegative than oxygen, it is expected that mesomeric form 2 should prevail relatively to mesomeric form 1, Scheme 2. This can nicely be observed in the crystal structure, since the C8–N18 bond has a length of 1.351 Å, indicating strong double bond character. A similar effect, double bond character and coplanarity of the structure, was reported for the case of a flavylium compound possessing a dimethylamino substituent in position 4′.[12]

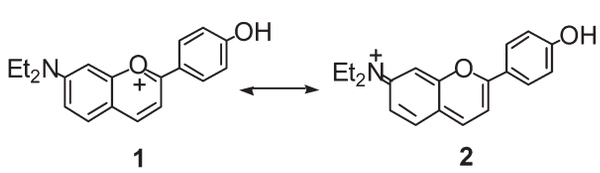

Scheme 2

Also worth of note in this structure is (i) the presence of an hydrogen bond between the hydrogen on O17 of the hydroxyl group in position 4′, and the fluorine atom F2 of the BF_4 counter ion, as well as, (ii) the existence of π–π stacking interaction between the flavylium molecules in the crystal packing, as revealed the distances less than 4 Å between the benzopyrylium rings.

Network of chemical reactions

According to Scheme 1, in acidic water (2 < pH < 7), it is possible to distinguish four species of this compound: the flavylium cation (**AH**$^+$); the quinoidal neutral base (**A**) formed upon deprotonation of **AH**$^+$; the hemiketal (**B2**) obtained by hydration of **AH**$^+$; the *cis*-chalcone (**Cc**) resulting from tautomerisation of **B2**; and the *trans*-chalcone (**Ct**) due to the

isomerization of **Cc**. At more acidic pH values the nitrogen of the amine can be protonated and thus $\mathbf{AH_2}^{2+}$ (at $[H^+] > 1$ M) and $\mathbf{B2}^+$, $\mathbf{Cc}^+$ and $\mathbf{Ct}^+$ (at pH < 2) can be formed. In basic aqueous solutions, ionized *cis* and *trans*-chalcones ($\mathbf{Cc}^-$ and $\mathbf{Ct}^-$, at pH > 8, $\mathbf{Cc}^{2-}$ and $\mathbf{Ct}^{2-}$, at pH > 9.2), can be obtained by deprotonation of the hydroxyl groups, and observed in the equilibrium or as transient species. Flavylium compounds are characterized by a pH dependent relative thermodynamic stability of the species that form the network, as well as by pH dependent kinetical response to external stimuli, *e.g.*, pH and light. In the case of the compound 7-(*N*,*N*-diethylamino)-4′-hydroxyflavylium, the following set of chemical equations can be used to characterize the network described by Scheme 1.

In acidic media:

$$\mathbf{AH}^+ \rightleftharpoons \mathbf{A} + H^+,\ K_a \quad (1)$$

$$\mathbf{AH}^+ + H_2O \rightleftharpoons \mathbf{B} + H^+,\ K_h \quad (2)$$

$$\mathbf{B} \rightleftharpoons \mathbf{Cc},\ K_t \quad (3)$$

$$\mathbf{Cc} \rightleftharpoons \mathbf{Ct},\ K_i \quad (4)$$

$$\mathbf{AH_2}^{2+} \rightleftharpoons \mathbf{AH}^+ + H^+,\ K_{a+} \quad (5)$$

$$\mathbf{BH}^+ \rightleftharpoons \mathbf{B} + H^+,\ K_{h+} \quad (6)$$

$$\mathbf{CcH}^+ \rightleftharpoons \mathbf{Cc} + H^+,\ K_{Cc+} \quad (7)$$

$$\mathbf{CtH}^+ \rightleftharpoons \mathbf{Ct} + H^+,\ K_{Ct+} \quad (8)$$

$$\mathbf{CtH}^+ \rightleftharpoons \mathbf{CcH}^+,\ K_{i+} \quad (9)$$

In basic media:

$$\mathbf{Cc} \rightleftharpoons \mathbf{Cc}^- + H^+,\ K_{Cc} \quad (10)$$

$$\mathbf{Cc}^- \rightleftharpoons \mathbf{Cc}^{2-} + H^+,\ K_{Cc-} \quad (11)$$

$$\mathbf{Ct} \rightleftharpoons \mathbf{Ct}^- + H^+,\ K_{Ct} \quad (12)$$

$$\mathbf{Ct}^- \rightleftharpoons \mathbf{Ct}^{2-} + H^+,\ K_{Ct-} \quad (13)$$

$$\mathbf{Cc}^- \rightleftharpoons \mathbf{Ct}^-,\ K_{i-} \quad (14)$$

$$\mathbf{Cc}^{2-} \rightleftharpoons \mathbf{Ct}^{2-},\ K_{i2-} \quad (15)$$

In Fig. 2, the pH dependent absorption spectra of equilibrated solutions of 7-(*N*,*N*-diethylamino)-4′-hydroxyflavylium, at extremely acidic pH values is shown, together with a photography of the colours involved.

The red form (λ_{max} = 528.5 nm) is the flavylium cation (AH^+), whose pH domain extends until the neutral region, see inset of Fig. 3. As shown by the crystal structure, there is a strong double bond character between the nitrogen and ring A. This suggests an extended conjugated system involving this atom and, by consequence, the appearance of the red colour, Scheme 2. In extremely acidic solutions ($pK_{a+} \sim -0.67$), the nitrogen is protonated and the conjugation is lost with a consequent shift to higher energies, leading to the yellow colour of the protonated flavylium, $\mathbf{AH_2}^{2+}$ (λ_{max} = 452 nm).

In Fig. 3, the spectra obtained *ca.* 3 min after a pH jump from solutions stored at pH = 1.0 to pH values in the range 2 < pH < 9 are shown. According to this figure, increasing pH leads to the disappearance of flavylium with concomitant formation of a new species, exhibiting a red shifted absorption band (λ_{max} = 574 nm), which can be assigned to the quinoidal base, **A**. As shown below, the quinoidal base **A** is then slowly transformed into the ionized chalcone species.

In order to confirm the existence of the four *trans*-chalcone species, a pH titration was carried out (Fig. 4), starting from $\mathbf{Ct}^{2-}$, obtained by dissolving the flavylium salt at pH = 12 and allowing the solution to equilibrate. The *trans*-chalcones $\mathbf{Ct}^{2-}$ and $\mathbf{Ct}^-$ dominate the basic region and are stable to carry out a normal titration procedure. However, at neutral and acidic pH values, where **Ct** and $\mathbf{Ct}^+$ are present, the spectra were collected immediately after a pH jump to avoid evolution of the system towards formation of flavylium cation. The absorption spectra are shown in Fig. 4a and the respective fitting in Fig. 4b.

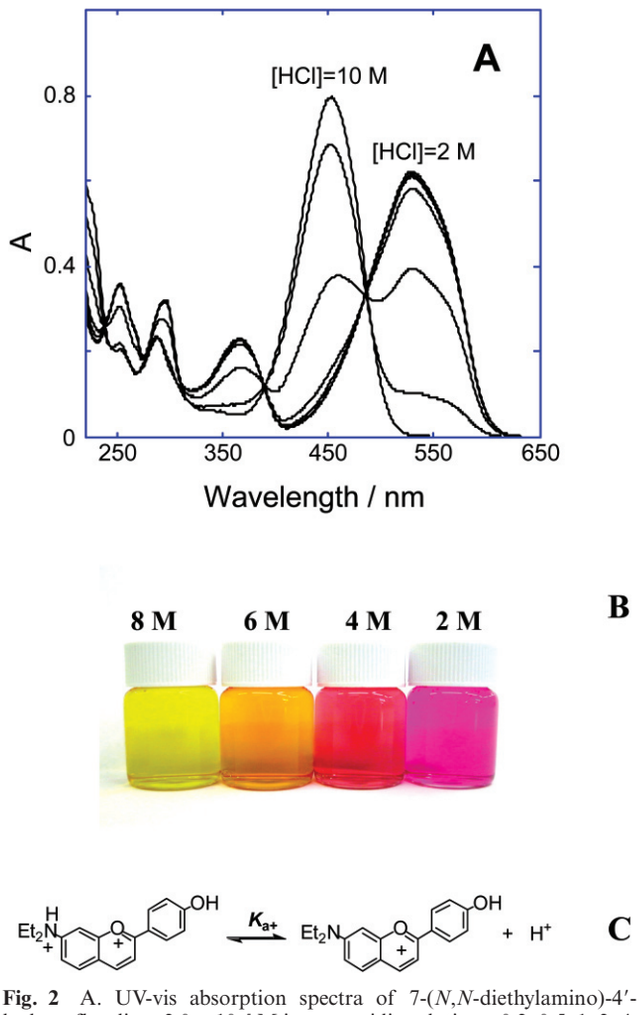

Fig. 2 A. UV-vis absorption spectra of 7-(*N*,*N*-diethylamino)-4′-hydroxyflavylium 2.0×10^{-5} M in very acidic solutions: 0.2, 0.5, 1, 2, 4, 6 and 10 M; B. colours of the solutions at different HCl concentrations; C. the equilibrium involved.

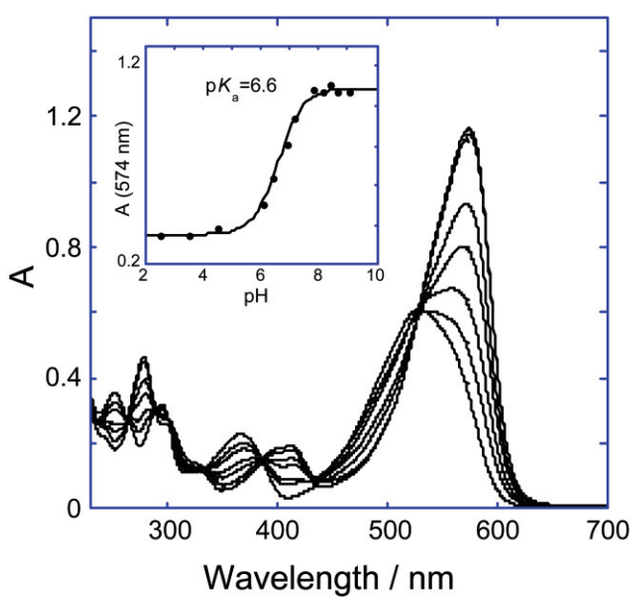

Fig. 3 Absorption spectra of 7-(*N*,*N*-diethylamino)-4′-hydroxyflavylium 2.0×10^{-5} M obtained ca. 3 minutes after a pH jump from 1 to 2 < pH < 9.

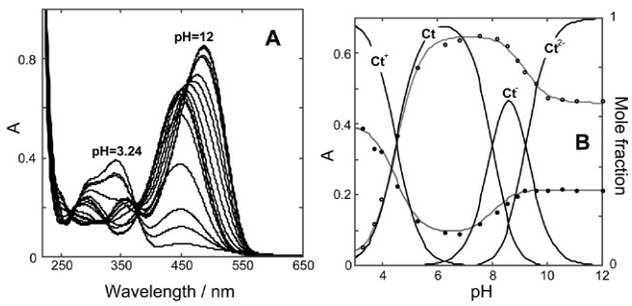

Fig. 4 A. Spectral variations of 7-(*N*,*N*-diethylamino)-4′-hydroxyflavylium 1.9×10^{-5} M obtained imediately upon pH jumps from equilibrated solutions at pH = 12.0 to pH values in the range 3 < pH < 12; B. Good fittings at 439 nm (○) and 344 nm (●) can be obtained considering four chalcone species with pK_a's of 9.2, 8.0 and 4.5.

The results are compatible with the existence of the species represented in eqns. (8), (12) and (13), leading to the following pK_a values: pK_{Ct+} = 4.5; pK_{Ct} = 8.0; pK_{Ct-} = 9.2.

Fig. 5 shows the pH dependent spectral variations that occur in equilibrated solutions (after *ca.* 1 d at room temperature), in the pH range 1.0–8.2. According to the mole fraction distribution of Fig. 4B, the chalcone species at pH 8.2 are mainly **Ct** and **Ct**$^-$, the absorption of this last one being slightly more intense and red shifted (λ_{max}(**Ct**$^-$) = 462 nm, λ_{max}(**Ct**) = 446 nm, see also Fig. 6). As long as the pH decreases, the **Ct** species (and at more acidic values, also **Ct**$^+$, λ_{max} = 342 nm) are transformed into the thermodynamically more stable species **AH**$^+$. Moreover, it may be concluded that for room temperature equilibrated solutions, at pH = 5.9 there is 50% of **Ct** and 50% of **AH**$^+$.

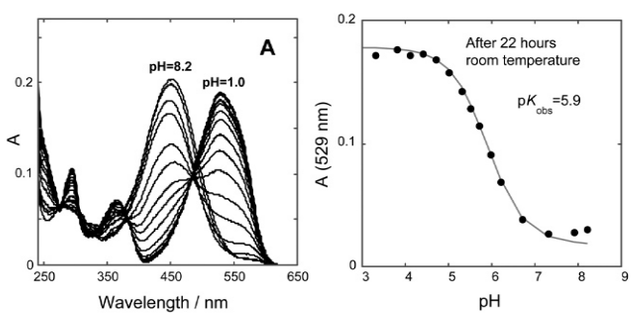

Fig. 5 pH dependent absorption spectra of 7-(*N*,*N*-diethylamino)-4′-hydroxyflavylium 6.7×10^{-6} M at room temperature, after 22 hours (A) and a fit of the absorbance at 529 nm (B). All the solutions were prepared from a stock solution at pH = 12.

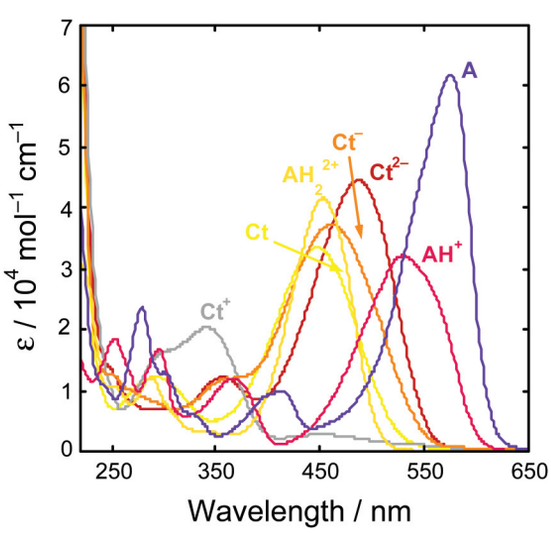

Fig. 6 Absorption spectra of some of the species detected in the chemical network of reactions originated by 7-(*N*,*N*-diethylamino)-4′-hydroxyflavylium in aqueous solutions.

In Fig. 6, the absorption spectra of the detected species of 7-(*N*,*N*-diethylamino)-4′-hydroxyflavylium are shown.

Thermodynamic energy level diagram

Before presentation and discussion of the kinetic processes of the network when it is perturbed by pH jumps, it is useful to construct an energy level diagram, like the one shown in Scheme 3. In this diagram, the free Gibbs energy, $\Delta G° = -RT\ln K_{eq}$, is represented for all species, following the same strategy as reported previously.[2] The pH dependent relative energy level of the species **AH**$^+$ and **A** is easily positioned taking into account eqn. (1). On the other hand, **AH**$_2^{2+}$ can be placed from **A**, using the sum of eqn. (1) with eqn. (5); in this case, the dependence on the proton concentration is quadratic. The data of Fig. 5 indicates that **Ct** should stay at the same energy level of **AH**$^+$ at pH = 5.9, allowing to position the *trans*-chalcone species. The remaining species can be positioned in energy using the protonation constants of the *trans*-chalcones.

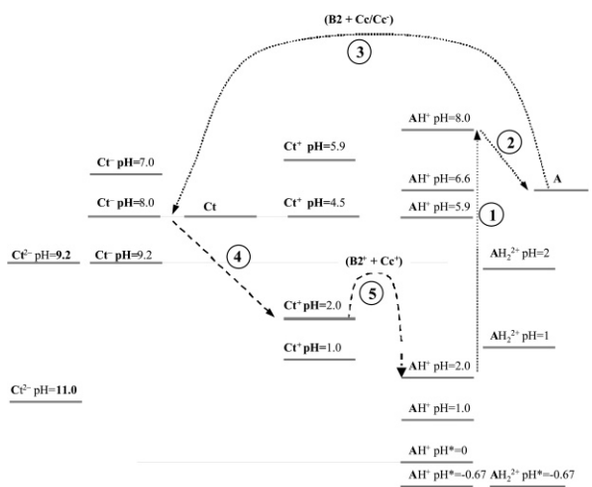

Scheme 3

Scheme 3 can account for the behaviour of the network of chemical reactions. For example, upon a pH jump from 2 to 8 (step 1) the species immediately formed is the quinoidal base **A** (step 2), according to Fig. 3. In a slower process, the species **A** is then transformed into the *trans*-chalcones, through **B2** and **Cc**/**Cc**$^-$, leading to a final situation at this pH value where *ca.* 50% of **Ct** and 50% of **Ct**$^-$ are present (step 3). If now a second pH jump back to pH = 2.0 is carried out, fast protonation of the *trans*-chalcones occurs, leading to **Ct**$^+$ (step 4). This last species evolves more or less rapidly (depending on pH, see below), into the final species **AH**$^+$ (step 5), most probably through **Cc**$^+$ and **B2**$^+$.

The chemical behaviour reported in Scheme 3 is an example of a pH driven cycle where the reverse reaction follows a different pathway from the forward reaction.

Kinetics of the network

The observed rate constants measured from forward and backward pH jumps are represented in Fig. 7 as a function of the final pH.

As discussed above, upon a pH jump from very acidic solutions to moderately acidic, or basic, pH values, the first species to be formed is the quinoidal base, **A**, which is reasonably stable when compared with other flavylium compounds lacking the amino substituent in position 4′ or 7.[16] This is due to the protection effect of the amines towards the hydration reaction: the strong electron donor ability of the amino group decreases the positive charge of the benzopyrylium system, slowing down the water attack to the flavylium cation. The reactivity of the species **A** increases at high pH values, where

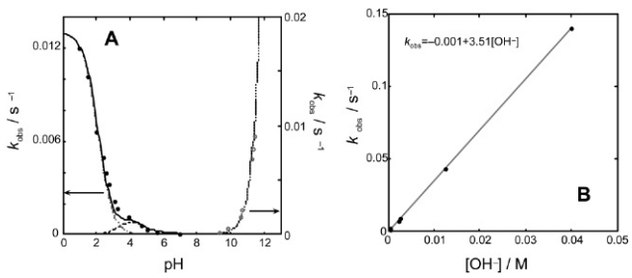

Fig. 7 A. Observed rate constants of the kinetic processes observed upon pH jumps from pH = 12 (●), and upon pH jumps from pH = 1.0 (○). The slower rate constants were measured following the changes in absorbance using a common spectrophotometer while faster processes were measured through a stopped flow apparatus. B. Linear dependence on the hydroxyl ion concentration was found for the observed rate constants in the basic region.

the hydroxyl ion attack becomes dominant. The process follows then a first order kinetics whose rate is equal to $3.5 \times [OH^-]\ s^{-1}$, Fig. 7B.

In a previous work,[17] a simple kinetic scheme, constituted by eqns. (1) and (16), was used to account for the behaviour of flavylium compounds possessing an hydroxyl in position 7,

$$\mathbf{AH^+} \underset{k_{-h}[H^+]}{\overset{k_h}{\rightleftharpoons}} \mathbf{X} \underset{k_{-i}}{\overset{k_i}{\rightleftharpoons}} \mathbf{Ct} \qquad (16)$$

where **X** is the intermediate state, constituted by **B** and **Cc** in fast equilibrium. Because **X** does not accumulate, its formation must be slower than its disappearance. This is possible if formation of **Ct** from $\mathbf{AH^+}$ (and **A**) is controlled by the hydration reaction that leads to **B**, and the back formation of $\mathbf{AH^+}$ (and **A**) from **Ct** is controlled by the *trans-cis* isomerization reaction. A kinetic treatment based on the steady state approximation for the intermediate species **X**, and considering that equilibrium (1) is by far the fastest process of the system, leads to eqn. (17).[18]

$$k_{obs} = \frac{[H^+]}{[H^+]+K_a}\frac{k_i k_h}{k_i + k_{-h}[H^+]} + \frac{k_{-i}k_{-h}[H^+]}{k_i + k_{-h}[H^+]} \qquad (17)$$

Representation of eq. (17) as a function of pH yields a bell-type shaped curve from which the rate constants can in principle be evaluated by a fitting procedure. In the present system, we verified that in the range $2 < pH < 6$ such kinetics is observed, Fig. 7A. The fitting can be achieved without ambiguity, for the following set of constants: $k_h = 1.5 \times 10^{-4}\ s^{-1}$, $k_{-i} = 1 \times 10^{-2}\ s^{-1}$, $k_i/k_{-h} = 5 \times 10^{-4}$ M.

However, there is a superposition of a second curve for $pH < 4$, clearly involving the amino protonated species. This behaviour is a result of the existence of the two different pathways reported in Scheme 3. The bell-type curve in the pH range $2 < pH < 6$ concerns steps (1) to (3). The second curve, at lower pH values, originates from steps (4) and (5). It is important to note that the first system is completely reversible in the pH range $4 < pH < 6$. In the case of the second system, there is no reversibility from $\mathbf{AH^+}$. In fact, when starting from $\mathbf{AH^+}$ the system goes through steps (1) to (3) and not (4) and (5).

The second system can be accounted for by eqns. (8) and (18), which are very similar to the previous system, without the reversibility in eqn. (16). The species **X′** is now constituted by $\mathbf{CcH^+}$ and $\mathbf{B2H^+}$ in fast equilibrium. Application of the steady state hypothesis to intermediate species **X′** leads to eqn. (19), from which the following set of constants could be obtained by a fitting procedure: $k_{i+}/k_{-h+} = 7.5 \times 10^{-3}$ M, and $k_{-i+} = 1.3 \times 10^{-2}\ s^{-1}$.

$$\mathbf{CtH^+} \underset{k_{i+}}{\overset{k_{-i+}}{\rightleftharpoons}} \mathbf{X'} \xrightarrow{k_{-h+}[H^+]} \mathbf{AH^+} \qquad (18)$$

$$k_{obs} = \frac{[H^+]}{[H^+]+K_{Ct+}}\frac{k_{-i+}k_{-h+}[H^+]}{k_{i+}+k_{-h+}[H^+]} \qquad (19)$$

Stopped flow

As described above, when a pH jump from solutions equilibrated at pH = 12 ($\mathbf{Ct^{2-}}$) is carried out to the neutral or acidic region, the species immediately formed are the *trans*-chalcones **Ct** or $\mathbf{Ct^+}$, depending on pH. In both cases, subsequent variations of the spectra can be observed; in particular, the $\mathbf{Ct^+}$ species gives rise to the flavylium cation as the thermodynamic product.

In order to clarify the nature of the spectral modifications occurring upon a pH jump from 12 to, for example, pH 7 (immediate **Ct** formation), the following series of pH jumps were carried out: (i) pH jump from solutions equilibrated at pH 12 to pH 7, (ii) the system was allowed to equilibrate for 1 h, (iii) a second pH jump to the acidic region was performed, and its kinetics followed by stopped flow. Fig. 8A shows the spectral variations of 7-(*N*,*N*-diethylamino)-4′-hydroxyflavylium upon step (iii). The inset of the figure clearly shows two kinetic processes, and the kinectic trace can be fitted with the sum of two exponentials with lifetimes of 0.5 s^{-1} and 0.0045 s^{-1}.

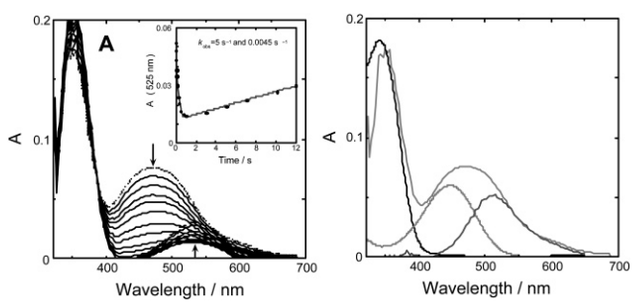

Fig. 8 A. Spectral variations observed on 7-(*N*,*N*-diethylamino)-4′-hydroxyflavylium upon a pH jump from 12 to 7 in order to form the species **Ct**, followed by a second pH jump to pH = 2.4, monitored by stopped flow; inset: fitting of the absorbance at 525 nm. B. The spectrum obtained after 8 ms is the sum of the contributions from the species $\mathbf{Ct^+}$, **Ct** and $\mathbf{Cc^+}$ (eventually $\mathbf{B2^+}$).

The results can be interpreted if an equilibrium between **Ct** and **Cc** (eventually also **B2**) is established at pH = 7, during step 2). When the second pH jump is performed, the species rapidly protonate, **Ct** giving $\mathbf{CtH^+}$, and **Cc** giving $\mathbf{CcH^+}$, a process which is too fast to be monitored by stopped flow. Inspection of Fig. 8A shows that immediately after the second pH jump, no flavylium is present at zero-time and thus the respective spectrum should be attributed to the absorptions of $\mathbf{Ct^+}$ and $\mathbf{Cc^+}$. The faster process observed, with a lifetime of 5 s^{-1}, can thus be assigned to the transformation of $\mathbf{Cc^+}$ (eventually in equilibrium with $\mathbf{B2^+}$) into $\mathbf{AH^+}$. The second decay, with a lifetime of 0.0045 s^{-1}, can be attributed to the transformation of $\mathbf{Ct^+}$ into $\mathbf{AH^+}$, through $\mathbf{Cc^+}$ (eventually in equilibrium with $\mathbf{B2^+}$) a process previously described in the discussion regarding Fig. 7.

In Fig. 8B attempts to obtain an absorption spectrum of the species involved, are shown. The spectrum obtained after 8 ms can be roughly fitted with a contribution of $\mathbf{Ct^+}$ (long trace line). The remaining absorption (short trace line), whose position is extremely red shifted, is attributed to a $\mathbf{Cc^+}$ species, eventually with a contribution from $\mathbf{B2^+}$, see below. Moreover, the percentage of *trans*-chalcone is 49%, in comparison with 51% of *cis*-chalcones, allowing to conclude that, at pH = 7.0, the equilibrium constant between **Ct** and **Cc** (eventually in fast equilibrium with **B2**) is 0.96, eqns. (3) and (4). There is however the unexpectedly red shifted absorption band of $\mathbf{Cc^+}$ species to be explained. In the following section, we present some arguments towards the possibility that this species is a tautomer in which the carbonyl group lies in position 9, instead of position 2.

Evidence for a tautomeric species

An interesting feature of this compound is the possibility of the protonated *cis*-chalcone to form a tautomeric species (Scheme 4) through an intramolecular proton transfer reaction.

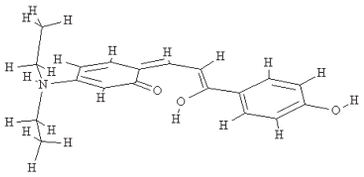

Scheme 4

The electronic transitions were calculated, for the protonated and unprotonated species of hemiketals and chalcones, with Hyperchem 5.0 (ZINDO/S, RHF level with CI of 99 single excited configurations), in optimized geometries (MM+). The **Cc**$^+$ tautomeric species is predicted to have a strongly red shifted absorption maximum (~130 nm) with respect to the initial **Cc**$^+$ tautomer, possessing the carbonyl in position 2 and the hydroxyl in position 9. A similar prediction (red shift) was obtained for the tautomer of Ct$^+$. The absence of any experimental evidence for the formation of a similar tautomeric species from **Ct**$^+$ must imply that the intermediate transition state in this isomer (achieved either by deprotonation of hydroxyl at position 9 or protonation of carbonyl at position 2) must be very hard to reach. In the case of the *cis* isomer, the possibility of a concerted mechanism involving a [1,7] sigmatropic rearrangent, makes the tautomerization possible.[18]

Unidirectional pH cycle

The present system can be used to introduce the concept of unidirectional pH cycle, Scheme 5. Let us take the example of the compound 4′,7-dihydroxyflavylium whose network of chemical reactions was previously reported in great detail, Scheme 5a).[11,18] Starting from the flavylium cation, **A**H$^+$, at pH = 1, and carrying out a direct pH jump up to 7, the final species formed is the *trans*-chalcone, **Ct**, which is obtained through the transient species (TS) **B2** and **Cc**. When a reverse pH jump back to 1 is carried out, the same transient species take place in the process. The cycle is completely reversible. In the case of a pH jump from 1 to 12, the transient species involved are those resulting from the attack of OH$^-$ to the quinoidal base **A**. In that case, **B2** is formed as the immediate result from OH$^-$ attack, but at higher pH values the species **B2**$^-$ and the correspondent ionized *cis*-chalcones should also be considered. Nevertheless, when the pH jump back to 1 is performed, the transient species are again **Cc** and **B2**. In the case of the compound 7-(*N*,*N*-Diethylamino)-4′-hydroxyflavylium, Scheme 5 b) if a pH jump starting from pH = 1 to pH = 7 takes place the process is identical to the previous one, quinoidal base being immediately obtained, and its slowly transformation into **Ct**, through the transient species **B2** and **Cc**. As in the case of 4′,7-dihydroxyflavylium a pH jump from 1 to 12, should involve the ionized hemiketal **B2** and the ionized *cis*-chalcones. However a great difference occurs when the back pH jump is carried out from 12 to 1. In this case there is a very rapid formation of the **Ct**$^+$ species, and the final species is the flavylium, but the transient species are necessarily **Cc**$^+$ and **B2**$^+$, which are different from those involved in the direct pH jumps.

Experimental section

Synthesis

7-(*N*,*N*-diethylamino)-4′-hydroxyflavylium tetrafluoroborate was prepared from condensation of 4-(diethylamino)-salicylaldehyde (1.9325 g, 10 mmol) and 4′-hydroxy-acetophenone (1.3615 g, 10 mmol), on the basis of a method described by Katritzky for similar compounds.[9] The reagents were dissolved in acetic acid (12.5 mL) and tetrafluoroboric acid (2.5 mL) was added. Acetic anhydride (10 mL) was then added, keeping the temperature below 60 °C (~10 min). The solution was stirred overnight. Addition of 25 mL of ethyl acetate leads to precipitation of a red solid that was filtered, washed with ethyl acetate, and dried in vacuum; 1,30 g (34%).

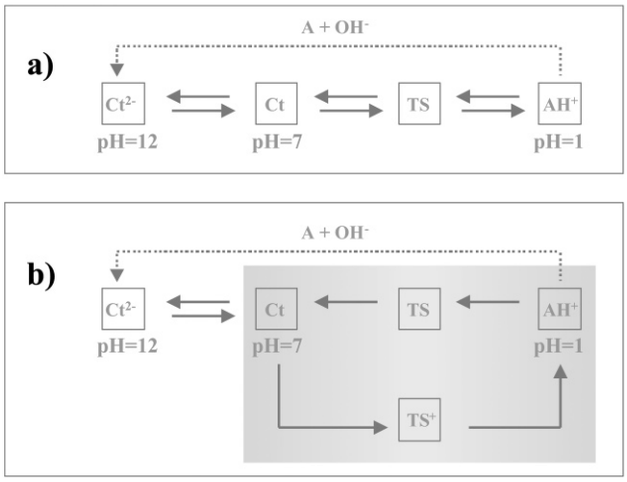

Scheme 5

The solid may be recrystallized from acetic acid, yielding violet needles with a beautiful greenish glow. Elemental analysis (Thermo Finnigan – CE Instruments EA 1112): exp. (calc. for $C_{19}H_{20}BF_4NO_2{\cdot}0.5H_2O$) %C 58.55 (58.49),%H 5.40 (5.42), %N 3.46 (3.59). EI-MS (HP 5988A): *m*/*z* 294.7 [M–BF_4^-]$^+$ (100%, M = $C_{19}H_{20}BF_4NO_2$). ^{1}H NMR (400 MHz, D_2O/DCl, pD < 0.6, 300 K): δ 0.99 (t, 6H, NCH_2CH_3, J = 6.9 Hz), 3.25 (q, 4H, NCH_2CH_3, J = 6.9 Hz), 6.29 (s, 1H, H8), 6.37 (d, 2H, H3′ + H5′, J = 8.4 Hz), 6.80 (d, 1H, H6, J = 9.2 Hz), 6.97 (d, 1H, H3, J = 8.0 Hz), 7.24 (d, 1H, H5, J = 9.2 Hz), 7.30 (d, 2H, H2′ + H6′, J = 8.4 Hz), 7.85 (d, 1H, H4, J = 8.0 Hz); (400 MHz, D_2O/NaOD, pD = 12.7, 300 K): δ 1.04 (t, 6H, NCH_2CH_3, J = 6.9 Hz), 3.26 (q, 4H, NCH_2CH_3, J = 6.9 Hz), 5.92 (s, 1H, H8), 6.14 (d, 1H, H6, J = 8.8 Hz), 6.55 (d, 2H, H3′ + H5′, J = 8.6 Hz), 7.39 (d, 1H, H3, J = 15.2 Hz), 7.48 (d, 1H, H5, J = 8.8 Hz), 7.82 (d, 2H, H2′ + H6′, J = 8.6 Hz), 8.05 (d, 1H, H4, J = 15.2 Hz)

General

All experiments were carried out in aqueous solutions. All chemicals were of analytical grade. The pH was adjusted by addition of HCl and NaOH to buffered solutions, and was measured in a Radiometer-Copenhagen PHM240 MeterLab potentiometer.

UV–vis absorption spectra were recorded in a Shimadzu UV2501-PC spectrophotometer.

Light excitation was carried out using a medium-pressure mercury arc lamp, and the excitation bands were isolated with interference filters (Oriel). The flash photolysis experiments were performed as previously described.[18]

The ^{1}H NMR experiments were recorded in a Bruker ARX-400 spectrometer operating at 400.13 MHz. The tetrafluoroborate salt of the flavylium was dissolved in D_2O, acidified with 20% (w/w) DCl, or basified with 40% (w/w) NaOD. The reported pD values are direct readings of the pH meter which can be corrected for the isotope effect through the equation pD = pH + 0.4.[19]

X-ray measurements

A red-green crystal of 7-(*N*,*N*-diethylamino)-4′-hydroxy-flavylium tetrafluoroborate was mounted on glass fiber using an epoxy resin and used for data collection.† Data were collected

† Crystal data. $C_{19}H_{20}NO_2BF_4$, M = 381.17, orthorhombic, a = 14.1926(7), b = 14.1055(9), c = 18.3190(11) Å, U = 3667.3(4) Å^3, T = 150(2) K, space group *Pbca* (no. 61), Z = 8, μ(Cu–Kα) = 0.989 mm^{-1}, 27 651 reflections measured, 3429 unique (R_{int} = 0.113). Final R indices (all data) R_1 = 0.0886 and wR_2 = 0.1975. CCDC reference number 242351. See http://www.rsc.org/suppdata/ob/b4/b409260k/ for crystallographic data in .cif or other electronic format.

at 150.0 K using an Enraf Nonius TurboCAD4 diffractometer. Monochromated Cu–Kα radiation was used throughout. The data were processed with HKL2000[20] and semi-empirical absorption correction was made using SORTAV.[21,22]

The structure was solved by direct methods using the program SIR-97[23] and refined by full-matrix least-squares methods on F^2 using SHELXL-97.[24] One of the ethyl groups exhibits orientational disorder, which was modeled using two sets of atomic sites with refined occupancies of 0.494 and 0.506; all other non-hydrogen atoms were refined anisotropically. Hydrogen atoms were placed geometrically and positional parameters were refined using a riding model. Atomic scattering factors were obtained with the use of International Tables for X-ray Crystallography.[25] Molecular graphics were obtained from ORTEP-3 for Windows[26] and the computing publication material from WinGX publication routines.[27]

Stopped-flow

The stopped flow experiments were performed in a SFM-300 spectrophotometer, controlled by a MPS-60 unit (Bio-Logic) and the data were collected by a TIDAS diode array (J&M), with wavelength range between 300 and 1100 nm, all connected to a computer. The standard cuvette has an observation path length of 1 cm. In these experiments, the dead time of each shot was previously determined to be 6.4 ms with a 7 mL s^{-1} flow rate.

Acknowledgements

Financial support by Fundação para a Ciência e Tecnologia (Portugal) and FEDER (project POCTI/QUI/47357/2002), as well as the European Community's Human Potencial Programme (D. Fernández) under contract HPRN-CT-2000-00029 [Molecular Level Devices and Machines] is acknowledged.

References

1 (*a*) J.-M. Lehn, in *Supramolecular Chemistry. Concepts and Perspectives*, VCH, Weinheim, 1994; (*b*) V. Balzani, F. Scandola, *Supramolecular Photochemistry*, Horwood, Chichester, 1991; (*c*) G. H. Brown, in *Photochromics*, Wiley, New York, 1971; (*d*) H. Dürr and H. Bouas-Laurent in *Photochromism—Molecules and Systems*, Elsevier, Amsterdam, 1990.
2 (*a*) F. Pina, M. Maestri and V. Balzani, in *Handbook of Photochemistry and Photobiology*, ASP, 2003, ch. 9, vol. 3, p. 411–449; (*b*) F. Pina, M. J. Melo, M. Maestri, R. Ballardini and V. Balzani, *J. Am. Chem. Soc.*, 1997, **119**, 5556–5561; (*c*) F. Pina, A. Roque, M. J. Melo, M. Maestri, L. Belladelli and V. Balzani, *Chem. Eur. J.*, 1998, **4**, 1184–1191; (*d*) F. Pina, M. J. Melo, M. Maestri, P. Passaniti and V. Balzani, *J. Am. Chem. Soc.*, 2000, **122**, 4496–4498.
3 A. P. De Silva and N. D. Mcclenagham, *Chem. Eur. J.*, 2004, **10**, 574–586.
4 M. Irie, *Chem. Rev.*, 2000, **100**, 1685–1716.
5 Y. Yokoyama, *Chem. Rev.*, 2000, **100**, 1717–1739.
6 (*a*) G. Berkovic, V. Krongauz and V. Weiss, *Chem. Rev.*, 2000, **100**, 1741–1753; (*b*) L. Eggers and V. Buss V, *Angew. Chem., Int. Ed. Engl.*, 1997, **36**, 881–883; (*c*) F. M. Raymo and S. Giordani, *J. Org. Chem.*, 2003, **68**, 1577–1585.
7 (*a*) R. A. McClelland and G. H. McGall, *J. Org. Chem.*, 1982, **47**, 3730; (*b*) J. R. Brouillard and J. E. Dubois, *J. Am. Chem. Soc.*, 1977, **99**, 1359; (*c*) R. A. McClelland and S. Gedge, *J. Am. Chem. Soc.*, 1980, **102**, 5838.
8 R. Robinson and D. D. Pratt, *J. Chem. Soc.*, 1922, 1577–1585.
9 A. R. Katritzky, P. Czerney, J. R. Levell and W. Du, *Eur. J. Org. Chem.*, 1998, 2623–2629.
10 P. Figueiredo, J. C. Lima, H. Santos, M. C. Wigand, R. Brouillard, A. L. Maçanita and F. Pina, *J. Am. Chem. Soc.*, 1994, **116**, 1249–1254.
11 L. Benedito, J. C. Lima, M. J. Melo, A. J. Parola, A. L. Maçanita and F. Pina, *Anal. Quím.*, 1997, **93**, 111–118.
12 A. Roque, C. Lodeiro, F. Pina, V. Balzani, M. Maestri, P. Passaniti and S. Dumas, *J. Am. Chem. Soc.*, 2003, **125**, 987–994.
13 M. C. Moncada, S. Moura, M. J. Melo, A. Roque, C. Lodeiro and F. Pina, *Inorg. Chim. Acta*, 2003, **356**, 51–61.
14 K. Ueno and N. Saito, *Acta Crystallogr., Sect B*, 1997, **B33**, 111.
15 A. Roque, C. Lodeiro, F. Pina, M. Maestri, R. Ballardini and V. Balzani, *Eur. J. Org. Chem.*, 2002, **16**, 2699–2709.
16 H. Wuncher, G. Haucke, P. Czerney and U. Kurzer, *J. Photochem Photobiol. A: Chem.*, 2002, **151**, 75–82.
17 F. Pina, M. J. Melo, L. Flamigni, R. Ballardini and M. Maestri, *New J. Chem.*, 1997, **21**, 969.
18 J. March, in *Advanced Organic Chemistry: Reactions, Mechanisms and Structure*, McGraw-Hill, London, 2nd edn., 1977, p. 1037.
19 P. K. Glasoe and F. A. Long, *J. Phys. Chem.*, 1960, **64**, 188.
20 Z. Otwinowski and W. Minor, *Methods Enzymol.*, 1997, **276**, 307–326.
21 R. H. Blessing, *Cryst. Rev.*, 1987, **1**, 3–58.
22 R. H. Blessing, *J. Appl. Crystallogr.*, 1989, **22**, 396–397.
23 SIR97: A. Altomare, M. C. Burla, M. Camalli, G. L. Cascarano, C. Giacovazzo, A. Guagliardi, A. G. G. Moliterni, G. Polidori and R. Spagna, *J. Appl. Crystallogr.*, 1999, **32**.
24 G. M. Sheldrick, *SHELXL-97, Program for refinement of crystal structures*, University of Göttingen, Germany, 1997.
25 *International Tables for X-ray Crystallography, vol. C*, ed Kluwer Academic Publishers, Dordrecht, The Netherlands, 1995.
26 L. J. Farrugia, *J. Appl. Crystallogr.*, 1997, **30**, 565.
27 L. J. Farrugia, *J. Appl. Crystallogr.*, 1999, **32**, 837–838.